ACS OMEGA

Article

Cite This: ACS Omega 2018, 3, 11788−11795

http://pubs.acs.org/journal/acsodf

Self-Assembled Polyvinyl Alcohol−Tannic Acid Hydrogels with Diverse Microstructures and Good Mechanical Properties

Ya-Nan Chen, Chen Jiao, Yaxin Zhao, Jianan Zhang, and Huiliang Wang*

Beijing Key Laboratory of Energy Conversion and Storage Materials, College of Chemistry, Beijing Normal University, Beijing, 100875, P. R. China

Supporting Information

ABSTRACT: Fabrication of hydrogels with unique microstructures and better mechanical properties through the self-assembly of commercially available synthetic polymers and small molecules is of great scientific and practical importance. A type of physical hydrogels is prepared by the self-assembly of polyvinyl alcohol (PVA) and tannic acid (TA) in aqueous solution with a low PVA−TA concentration (0.5−6.0 wt %) at room temperature. With the increase of the PVA−TA concentration, the water content of the hydrogels increases, and the content of TA in the hydrogels decreases from 23.1 to 6.4%. The driving force for the self-assembly is proven to be the hydrogen bonding between PVA and TA, which also induces the crystallization of PVA chains. The self-assembled PVA−TA hydrogels have diverse morphologies that change from microspheres to oriented porous structures with the increase of the PVA−TA concentration, and these structures are all composed of nanosized particles, fibers, and/or sheets. Most of the self-assembled PVA−TA hydrogels show good mechanical properties. The highest tensile strength and elastic modulus of the PVA−TA hydrogel prepared with 1.0 wt % PVA−TA concentration are about 84 and 30 kPa, respectively. This self-assembly method would lead to the fabrication of more hydrogels with unique microstructures and properties for practical applications.

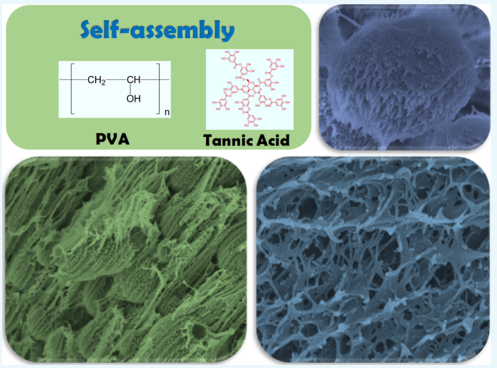

1. INTRODUCTION

As a typical type of wet and soft materials, hydrogels are three-dimensionally cross-linked polymeric networks that can absorb a large portion of water while maintaining their solidlike shapes. Because of their high-water absorption, high permeability to small molecules, similarity to biological soft tissues, and stimuli-responsive properties in some cases, hydrogels have been used in many fields, such as water-retention materials, biomaterials, sensors, actuators, and so forth.[1−3] Most synthetic hydrogels are synthesized by polymerizing hydrophilic monomer(s) in the presence a chemical cross-linking agent. Certainly, some physical interactions such as hydrogen bonding (H bonding) and chain entanglement also take part in the cross-linking and contribute to the mechanical properties of the chemical hydrogels.[4] On the other hand, biological hydrogels are usually physically cross-linked by H bonding and electrostatic interactions.[5,6] More importantly, they also have anisotropic and hierarchical structures because of the self-assembly of biomacromolecules driven by the physical interactions.[7] There is an increasing interest in developing biomimetic hydrogels constructed and toughened by physical interactions.

Many kinds of self-assembled hydrogels have been reported. The self-assembled hydrogels are commonly made with small organic molecules (gelators),[8,9] graphene (or reduced graphene oxide) with inorganic materials,[10−12] and more often biomolecules, such as peptide,[13−16] proteins,[17−20] DNA[21−23] and RNA,[24] liposomes,[25] alginates,[26] and so forth. To our knowledge, there are very few reports on hydrogels made by the self-assembly of commercially available synthetic polymers and small molecules.[27] The driving forces for the self-assembly include H bonding, electrostatic interaction (ionic bonding), hydrophobic interaction, $\pi-\pi$ interaction, coordination, and so forth. The self-assembled hydrogels made with biomacromolecules generally show a microstructure of interconnected nanofibers (fibrils).[28,29] Moreover, the self-assembled biomacromolecular hydrogels usually possess poor mechanical properties. The reported mechanical properties of the hydrogels are mostly the shear storage moduli measured with rheological tests, which are mostly less than 1 kPa,[14,30,31] with the highest around 100 kPa,[32] whereas the tensile mechanical properties of the self-assembled hydrogels are rarely reported. Therefore, facile fabrication of hydrogels with unique microstructures and better mechanical properties through the self-assembly of commercially available synthetic polymers and small molecules is of great scientific and practical importance.

Received: August 14, 2018
Accepted: September 10, 2018
Published: September 24, 2018

DOI: 10.1021/acsomega.8b02041
ACS Omega 2018, 3, 11788−11795

To enable the self-assembly, polymers and small molecules that can form strong H bonding and/or other physical interactions need to be used. Here, we chose polyvinyl alcohol (PVA) and tannic acid (TA), which act as both H-bonding donor and acceptor, as the raw materials. PVA hydrogel is one of the very few synthetic hydrogels that are totally physically cross-linked. PVA hydrogels are commonly prepared with the classic freezing−thawing method, and the physical cross-links include crystallization of PVA and H bonding between PVA chains that are formed during the freezing process.[33,34] TA is a natural polyphenolic compound composed of five digallic acid units attached to a central glucose core.[35] Because of the presence of a large number of phenolic and carbonyl groups, TA can form different types of interactions such as hydrogen bonding, ionic bonding, and hydrophobic interactions with many small molecules and polymers. It has been widely used in the layer-by-layer assembly technique to prepare self-assembled thin layers with polymers such as poly(vinyl pyrrolidone),[36−38] poly(*N*-vinylcaprolactam),[39] and polyethylene glycol.[40] TA has also been applied to prepare hydrogels by H bonding with polymers.[41,42] Shin et al.[43] reported a DNA/TA hydrogel in which TA plays a role as a "molecular glue" by reversibly connecting between phosphodiester bonds via H bonding. Fan et al.[44] fabricated TA-based supramolecular hydrogels by utilizing H bonding and ionic bonding in the presence of Fe(III) ions between TA and several commercially available water-soluble polymers. Several types of PVA−TA hydrogels have also been reported. For example, Liu and co-workers[45] reported a multinetwork physical hydrogel named TA−PVA/BSA (bovine serum albumin), in which TA cross-links with BSA proteins and PVA chains through H bonding and hydrophobic interactions. Hong[46] reported a PVA−TA hydrogel for wound dressing applications by a freezing−thawing process. Our group[47] also reported a PVA−TA hydrogel with excellent mechanical properties and shape memory behaviors, in which the stronger H bonding between PVA and TA and the weaker H bonding among PVA chains act as the "permanent" and "temporary" cross-links, respectively. These PVA−TA hydrogels are generally prepared by the freezing−thawing method and/or the assistance of coordination with Fe(III) ions. No PVA−TA hydrogels have been prepared with a self-assembly method without the assistance of freezing and the addition of metal cations.

In this work, we prepared a PVA−TA hydrogel by the H bonding-driven self-assembly at room temperature. The obtained PVA−TA hydrogels exhibit diverse microstructures and good mechanical properties.

2. RESULTS AND DISCUSSION

2.1. Hydrogel Preparation and Characterization. The PVA−TA hydrogels were prepared with a self-assembly method. First, PVA and TA with a fixed mass ratio of 9:1 were dissolved in water under heating and mechanical stirring till the formation of homogeneous aqueous solutions. Note that at a high PVA−TA concentration, PVA and TA coagulate to form inhomogeneous solutions; so the PVA−TA concentration was chosen in the range of 0.5−6.0 wt % to ensure homogeneous solutions. Then, the solutions were kept still in an incubator at 25 °C for 5−7 days. PVA and TA did not precipitate from the solutions immediately when the solutions were cooled to room temperature. Instead during the standing, a layer of solidlike materials (i.e., hydrogels) was gradually formed on the bottom of the beakers, leaving a clear liquid in the major upper layer. The final thickness of the hydrogel depends on the PVA−TA concentration and the depth of the solution. As no additional chemicals or external forces are applied to the gel formation process, the hydrogels are formed by the self-assembly of PVA and TA molecules. The formation of self-assembled structures and the driving forces for them will be proven in the following parts.

Because the homogeneous aqueous PVA−TA solutions did not completely transform into hydrogels, the water contents (WCs) of the PVA−TA hydrogels were significantly lower than the calculated theoretical values (94−99.5%) from the feeding ratios. The measured WCs of the PVA−TA hydrogels prepared at different PVA−TA concentrations are shown in Figure 1. With the increase of the PVA−TA total concentration, the WC of the PVA−TA hydrogels increased from 78.4 to 88.5 wt %.

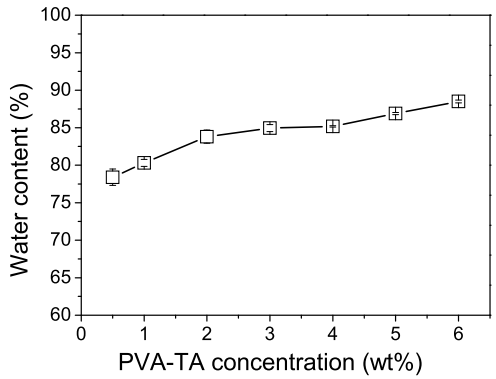

Figure 1. WCs of the PVA−TA hydrogels as a function of the PVA−TA concentration.

The composition of the PVA−TA hydrogels may also be different from the feeding mass ratio (9:1). To obtain the actual compositions of the PVA−TA hydrogels, elemental analyses were carried out. PVA and TA have significantly different contents of the hydrogen element, and they are 9.15 and 3.08%, respectively. As shown in Figure 2a, with the increase of the PVA−TA concentration, the hydrogen element contents of the PVA−TA hydrogels increase from 7.75 to 8.76%. By simple arithmetic calculations, the real solid contents of PVA and TA in the PVA−TA hydrogels prepared at different PVA−TA concentrations are obtained. As shown in Figure 2b, with the increase of the PVA−TA concentration, the content of PVA gradually increases from 76.9 to 93.6%, whereas the content of TA simultaneously decreases from 23.1 to 6.4%. These results indicate that there is more TA in the hydrogels prepared at a low total PVA and TA concentration (<4.0 wt %) than the feeding ratio (10 wt %) while less at a higher PVA and TA concentration. The possible reason is the competition between H bonding among PVA chains and that between PVA and TA. At a higher PVA−TA concentration, the close contact of PVA chains leads to the easier formation of H bonding among them and hence possibly the formation of more PVA crystallites (this will be proven in the following part), which prevents the formation of H bonding between PVA and TA.

Our previous work has proven that strong H bonding is present in the tough, shape memory PVA−TA hydrogels.[47] The PVA−TA hydrogels in this work are prepared with a different method and at much lower concentrations of PVA

DOI: 10.1021/acsomega.8b02041
ACS Omega 2018, 3, 11788−11795

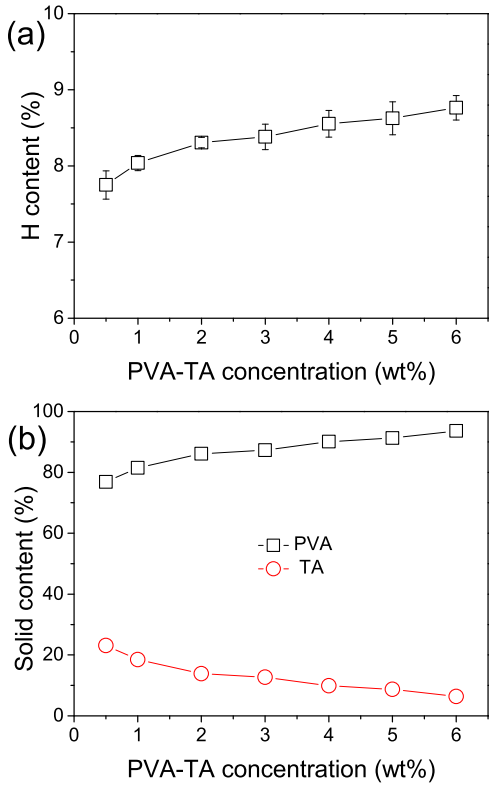

Figure 2. Change of the hydrogen element contents (a) and PVA and TA solid contents (b) in the PVA–TA hydrogels with the PVA–TA concentration.

and TA. Attenuated total reflectance–Fourier transform infrared (ATR–FTIR) characterizations of pure PVA and TA and dried PVA–TA hydrogels were performed to prove the presence of H bonding between PVA and TA. As shown in Figure 3, the broad and strong absorption bands at 3276 and

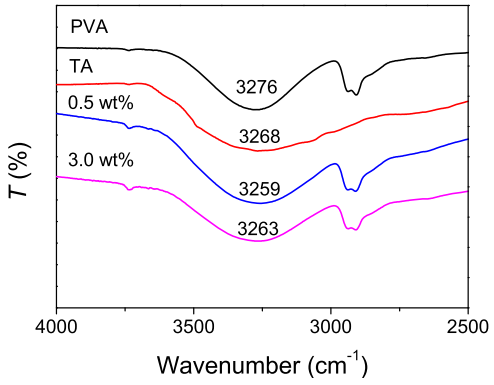

Figure 3. ATR–FTIR spectra of pure PVA and TA and dried PVA–TA hydrogels obtained at a PVA–TA concentration of 0.5 and 3.0 wt %.

3268 cm^{-1} in the spectra of PVA and TA are attributed to the symmetrical stretching vibration of hydroxyl (–OH) groups, respectively. However, the –OH stretching peaks of the PVA–TA hydrogels at the PVA–TA concentrations of 0.5 and 3.0 wt % are shifted to a lower wavenumber of 3259 and 3263 cm^{-1}, respectively. It is well-known that the formation of intra- or intermolecular H bonding reduces the force constants of the chemical bonds, leading to a shift to lower wavenumbers of their vibrational frequencies.[48] We can speculate that the H bonding exists between PVA and TA.

As is well-known, PVA is a semicrystalline polymer, and crystallites are present in PVA solids and the hydrogels prepared solely or mainly with PVA. As shown in Figure 4, the

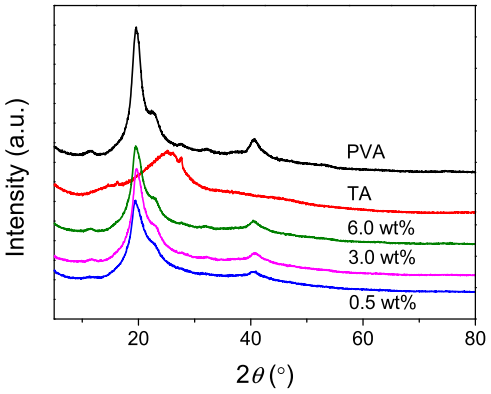

Figure 4. XRD patterns of PVA, TA, and PVA–TA hydrogels obtained at 25 °C at a PVA–TA concentration of 0.5, 3.0, and 6.0 wt %.

X-ray diffraction (XRD) pattern of the PVA solid shows three typical peaks at 2θ = 19.6°, 22.9°, and 40.8°, corresponding to the (101), (200), and (102) planes of PVA crystallites.[49] The XRD pattern of TA shows a blunt peak centered at 2θ = 26.1° rather than the obvious sharp peaks of crystalline structures, which indicates the amorphous nature of TA. The PVA–TA hydrogels show similar XRD patterns as PVA, suggesting the presence of PVA crystallites. For the PVA–TA hydrogels prepared with a PVA–TA concentration of 0.5, 3.0, and 6.0 wt %, their crystallinities are 25.58, 26.39, and 30.98%, respectively, lower than the crystallinity of PVA (38.05%). The results reveal that the addition of amorphous TA leads to the decreased crystallinities of the hydrogels. The increased crystallinity of the PVA–TA hydrogels with increasing concentration of PVA and TA is consistent with the increase of PVA content in the hydrogels (Figure 2b).

It is necessary to note that no PVA crystallites are present in the PVA–TA hydrogels reported in our previous work[47] because of the fast formation of H-bonded PVA–TA aggregates at a high PVA–TA concentration (>10 wt %) even during the mixing at a high temperature, whereas at a low PVA–TA concentration, no obvious large aggregates are formed when PVA and TA are mixed at a high temperature. Only when the solutions are cooled to room temperature and stood for a long time (days), a layer of solidlike material containing PVA crystallites is gradually formed. It is also necessary to mention that blank PVA solutions without TA cannot crystallize and hence transform into hydrogels after a long standing time (months) at room temperature, even at a high PVA concentration. Therefore, it is reasonable to conclude that TA facilitates the crystallization of PVA chains, and the possible reason is that the formation of H bonding between PVA and TA leads to the approaching and aggregation of PVA chains, which enables the proper conformations required for their crystallization. On the other hand, the formation of H bonding between PVA and TA decreases the ratio of PVA that can crystallize and hence the lowered crystallinity of the gels prepared at a low PVA–TA concentration.

DOI: 10.1021/acsomega.8b02041
ACS Omega 2018, 3, 11788–11795

In summary, the driving force for the self-assembly is essentially the H bonding between PVA and TA, and it also induces the crystallization of PVA chains.

2.2. Morphologies of Hydrogels. Figures 5 and S1 show that the hydrogel prepared at a PVA−TA concentration of 0.5

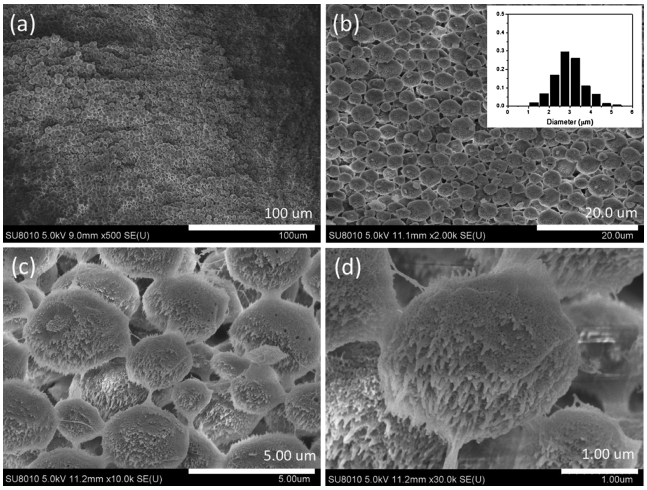

Figure 5. SEM images and the particle size distribution (inset in b) of the PVA−TA hydrogel obtained at a PVA−TA concentration of 0.5 wt % at 25 °C. Scale bars: 100 (a), 20 (b), 5 (c), and 1 μm (d).

wt % is completely composed of microspheres. The size distribution of the microspheres is shown in the inset of Figure 5b. The diameter of the microspheres is in the range of about 1−5 μm, mainly around 3 μm. A detailed examination shows that the microspheres are linked together by fibers (Figure 5c), and the microspheres are composed of nanoparticles with many short nanofibers on their surfaces (Figure 5d).

With the increase of the PVA−TA concentration, the morphology of the hydrogels changes, and significant differences are found between the upper and lower layers of the gels. At the PVA−TA concentration of 1.0 wt %, the hydrogel still shows the microstructure of microspheres. On comparison to the microspheres obtained at 0.5 wt %, we find that the microspheres become bigger, and those in the lower layer (mostly 6−8 μm, Figure 6a2) are bigger than those in the upper layer (mainly 4−5 μm, Figure 6a1) of the gel. The microspheres are also composed of nanoparticles with many short nanofibers on their surfaces (Figure S2). When the PVA−TA concentration is increased to 2.0 wt %, the size of the microspheres increases to be around 10 μm in the upper layer of the gel (Figure 6b1). Microspheres can also be found in the lower layer, but the number of microspheres decreases significantly, whereas many nanosized sheets or meshes appear (Figure 6b2). For the hydrogel prepared at a PVA−TA concentration of 4.0 wt %, microsphere-like structures can still be found in the upper layer, but the main morphology is oriented nanosized sheets and meshes (Figures 6c1 and S3a). In the lower layer, no microspheres can be found, instead, a more dense and continuous oriented porous structure appears (Figure 6c2). Magnification of the microsphere-like structures and the porous structure indicates that they are composed of nanosized fibers (Figures 6c3,c4 and S3b). At the highest concentration of PVA−TA studied, no significant difference is found in the morphologies between the upper and lower layers of the gel, the whole gel shows a porous structure with a pore size less than 1 μm, and the pore walls are composed of

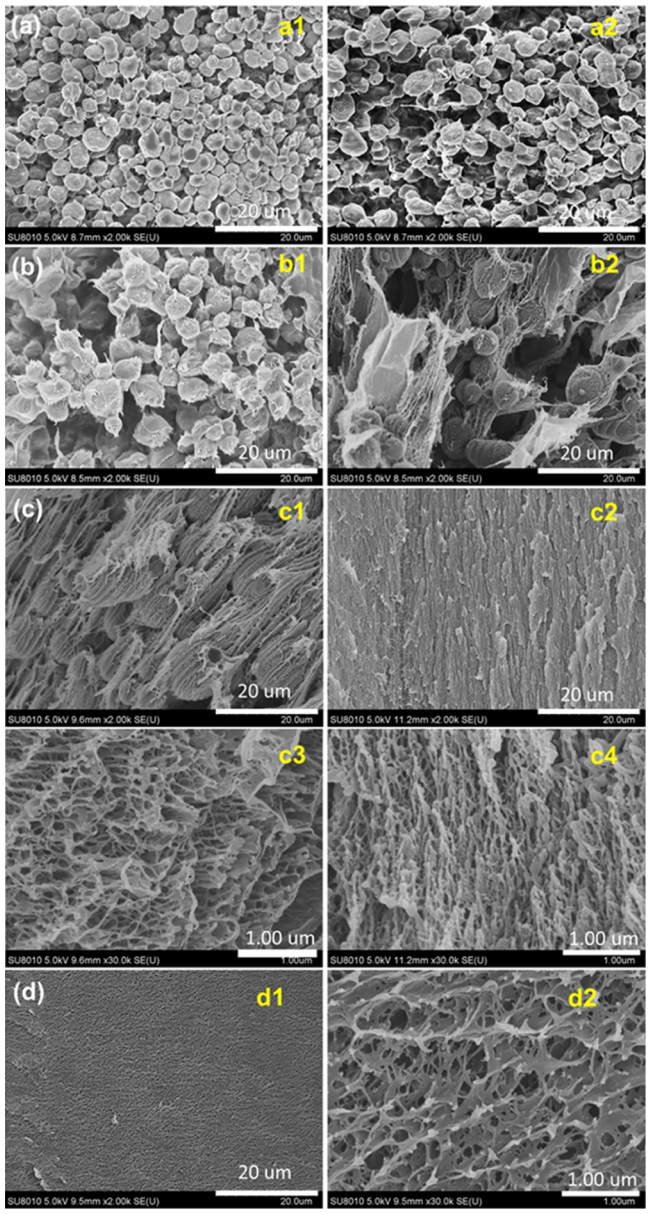

Figure 6. SEM images of the PVA−TA hydrogels obtained at a PVA−TA concentration of 1.0 (a), 2.0 (b), 4.0 (c), and 6.0 wt % (d) at 25 °C. (a1,b1,c1) are of the upper layer and (a2,b2,c2) are of the lower layer of the gels; (c3,c4,d2) are the magnification of the corresponding (c1,c2,d1), respectively.

nanosized sheets and fibers (Figure 6d), similar to that of the PVA−glycerol supramolecular hydrogel.[50]

We have also prepared PVA−TA hydrogels (0.5 wt %) under different conditions and examined their morphologies.

2.2.1. Cooling treatment. The homogeneous PVA−TA solution was cooled at 0 °C (ice-water bath) for 30 min before it was left to stand at room temperature. The morphology of the resulted PVA−TA hydrogels is displayed in Figure 7a,b. With comparison to that without the cooling treatment (Figure 5a,b), the number of microspheres dramatically increases, but the size of the microspheres significantly decreases. The diameters of the microspheres are in the range of 0.6−2.4 μm, mainly around 1.3 μm (inset in Figure 7a). The cooling of the PVA−TA solution at a low temperature facilitates the

DOI: 10.1021/acsomega.8b02041
ACS Omega 2018, 3, 11788−11795

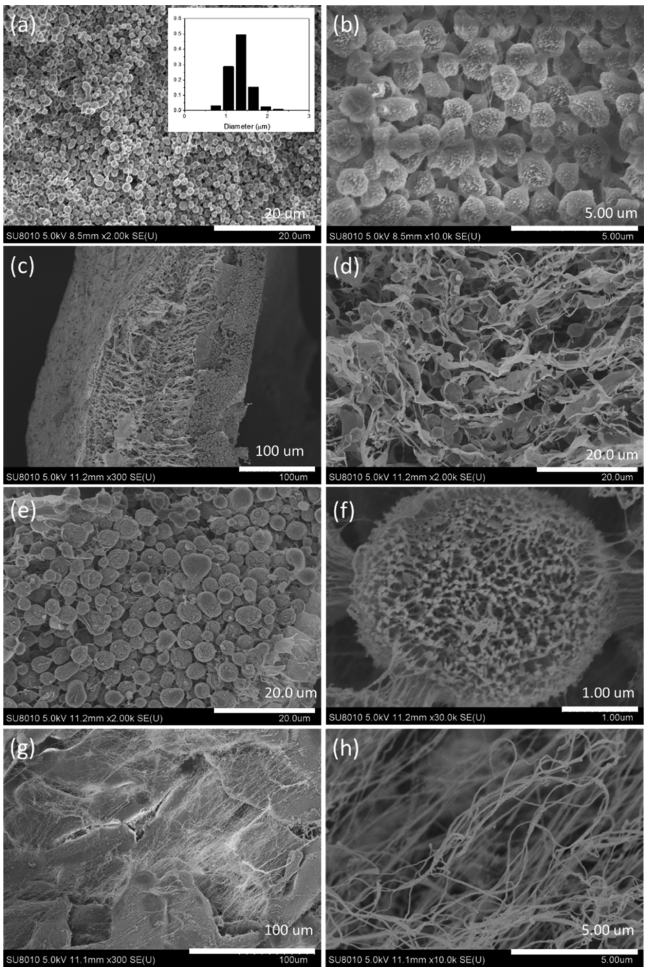

Figure 7. SEM images of the PVA−TA hydrogels (0.5 wt %) prepared under different conditions. (a,b) Being cooled at 0 °C for 30 min before setting at room temperature, the inset in (a) shows the particle size distribution; (c−f) with the addition of 1×10^{-3} M SDBS; (g,h) with mechanical stirring.

formation of H bonding among PVA chains and hence the crystallization of PVAand the formation of more microspheres.

2.2.2. Addition of a surfactant. A low concentration of the surfactant sodium dodecyl benzene sulfonate (SDBS) (1×10^{-3} M) was added into the PVA−TA solution (0.5 wt %), and the microstructure of the resulted PVA−TA hydrogel is displayed in Figure 7c−f. Note that there is a significant difference in the morphologies between the lower and upper layers of the hydrogel. The lower layer shows a loose and porous structure. Not only microspheres but also microsized sheets with a thickness in nanometers are found in the lower layer (Figure 7d). The upper layer is mostly composed of microspheres with a diameter around 3−4 μm (Figure 7e). The microspheres are different from those microspheres formed without the addition of SDBS, they show a loose porous structure consisted of nanofibers, and the microspheres are also connected by nanofibers (Figure 7f). Similarly, at the PVA−TA total concentration of 1.0 wt %, more nanosheets rather than dense microspheres were observed in the presence of SDBS (Figure S4). These scanning electron microscopy (SEM) investigations suggest that the addition of the surfactant SDBS inhibits the formation of dense microstructures by preventing the aggregation of nanoparticles.

2.2.3. Mechanical agitation. Mechanical stirring was applied to the solution in the first 24 h during the setting at room temperature. In this case, no microspheres appear anymore. Instead, the main microstructures of the hydrogel are large and thick sheets or clusters as well as very long (up to several tens micrometers) and thin (with diameters less than 100 nm) fibers (Figure 7g,h). The mechanical agitation leads to the coagulation of PVA and TA, so it also prevents the aggregation of nanoparticles into microspheres.

These SEM observations show that the self-assembled PVA−TA hydrogels have diverse morphologies that change from microspheres to oriented porous structures with the increase of the PVA−TA concentration, and these structures are all composed of nanosized particles, fibers, and/or sheets. The formation mechanism of these morphologies can be explained as follows: the formation of H bonding between PVA and TA leads to their aggregation and crystallization of PVA chains inside the aggregates, forming nanosized particles. At a very low PVA−TA concentration, the aggregation and merging of the nanoparticles in the liquid phase lead to the formation of large microsized particles (microspheres) that can precipitate from the solutions to form a hydrogel. When the PVA−TA concentration is increased, the easier formation of H bonding between PVA and TA leads to the formation of more nanoparticles that can merge into fibers or sheets. Under the effect of gravity, the fibers or sheets precipitate layer by layer, forming hydrogels with oriented porous structures.

2.3. Mechanical Properties of Hydrogels. Most of the self-assembled PVA−TA hydrogels show good mechanical properties. The tensile mechanical properties of the PVA−TA hydrogels prepared with different PVA−TA concentrations were measured, and the typical tensile stress−strain (σ_t−ε_t) curves are displayed in Figure 8; the tensile strength (σ_b) and elastic moduli (E) of the PVA−TA hydrogels are summarized in Figure 8b. Note that the PVA−TA hydrogel prepared with

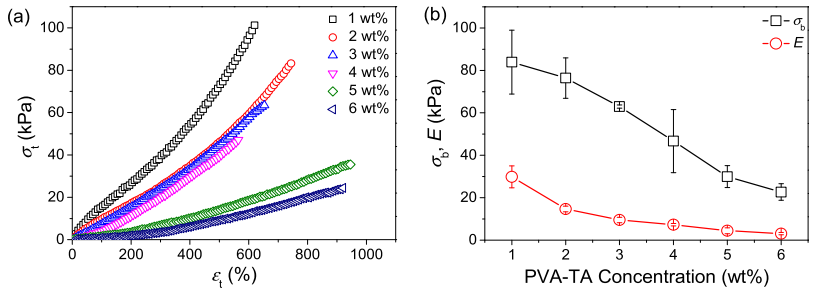

Figure 8. Typical tensile stress−strain curves of the PVA−TA hydrogels prepared with different PVA−TA concentrations (a) and their tensile (σ_b) and elastic moduli (E) (b).

DOI: 10.1021/acsomega.8b02041
ACS Omega 2018, 3, 11788−11795

0.5 wt % PVA−TA concentration was too weak to be tested. The other hydrogels show high elongations (ε_b) in the range of 565−950%. The PVA−TA hydrogel prepared with 1.0 wt % PVA−TA concentration has the highest σ_b and E values, and they are about 84 and 30 kPa, respectively. With the increase of PVA−TA concentration, both σ_b and E gradually decrease, in accordance with the increasing WC and the decreasing content of TA in the gels.

Note that the mechanical properties of the self-assembled PVA−TA hydrogels are inferior to those of PVA−TA hydrogels prepared by the mixing method.[47] The possible reasons are the presence of less H bonds between PVA and TA in the self-assembled PVA−TA hydrogels (as there is a significant portion of PVA participates in forming crystallites) and the weak interactions between the nanosized and/or microsized structures.

3. EXPERIMENTAL SECTION

3.1. Materials. PVA with an alcoholysis degree of 99% (M_n: 7.7 × 10^4) was purchased from Sinopharm Chemical Reagent Co., Ltd. (Shanghai, China); TA ($C_{76}H_{52}O_{46}$, A. R. grade) was purchased from Shanghai Macklin Biochemical Co., Ltd. (Shanghai, China); and SDBS ($C_{18}H_{29}NaO_3S$, A. R. grade) was purchased from Tianjin Damao Chemical Reagent Factory (Tianjin, China). The chemicals were not further purified, and deionized water was used for the hydrogel preparation.

3.2. Preparation of Hydrogels. PVA and TA with a fixed mass ratio of 9:1 at a total concentration from 0.5 to 6.0 wt % were dissolved in 90 °C deionized water with the assistance of mechanical agitation for 2 h. The resultant homogeneous solutions were transferred into beakers preheated to 90 °C, and then the sealed beakers were placed in an incubator at 25 °C for several days. During this period, a layer of PVA−TA hydrogel was formed at the bottom of the beakers.

WCs of the PVA−TA hydrogels were calculated as follows

$$\mathrm{WC} = (m_{\mathrm{wet}} - m_{\mathrm{dry}})/m_{\mathrm{wet}} \times 100\%$$

where m_{wet} and m_{dry} are the weights of the as-prepared and the dried gel samples, respectively.

3.3. Characterization. Elemental analyses of PVA−TA hydrogels were recorded on a varioELcube element analyzer (Elementar, Germany). ATR−FTIR spectra were recorded on a Nicolet FTIR 6700 spectrometer (Thermo Electron Scientific Instruments Corp., USA). XRD patterns of the hydrogels and raw materials were recorded with a PANalytical-X'Pert PRO diffractometer (PANalytical Co. Ltd., Netherlands) using Cu Kα radiation. The PVA−TA hydrogel samples for SEM observations were first frozen with liquid nitrogen for about 5 min and then freeze-dried with an LGJ-10C vacuum freeze dryer (Beijing Sihuan Scientific Instrument Factory, China) for about 48 h. The freshly cracked cross-sections of the freeze-dried gel samples were observed with a scanning electron microscope (Hitachi S-8010, Japan) with an accelerating voltage of 5 kV.

3.4. Tensile Mechanical Tests. Tensile testing method was the same as that used in our previous work.[47] Tests were performed on standardized dumbbell-shaped gel specimens by using an Instron 3366 electronic universal testing machine (Instron Corporation, MA, USA) at a cross-head speed of 100 mm/min. Tensile stress (σ_t) and tensile strain (ε_t) are defined as usual, and tensile strength (σ_b) and elongation (ε_b) are σ_t and ε_t when the specimen breaks. The initial elastic modulus (E) was calculated in the linear stress and strain range between ε_t = 10 and 35%.

4. CONCLUSIONS

In summary, we have successfully prepared PVA−TA hydrogels through a self-assembly method performed at low PVA−TA concentrations at room temperature. The H bonding between PVA and TA is essentially the driving force for the self-assembly, and it also induces the crystallization of PVA chains. The self-assembled PVA−TA hydrogels have diverse morphologies that change from microspheres to oriented porous structures with the increase of the PVA−TA concentration, and these microstructures are all composed of nanosized particles, fibers, and/or sheets. The PVA−TA hydrogels also show good mechanical properties. We believe that the H bonding-driven self-assembly method can be expanded to the preparation of many other physical hydrogels, and these hydrogels with unique microstructures and properties will have many application prospects.

■ ASSOCIATED CONTENT

Supporting Information

The Supporting Information is available free of charge on the ACS Publications website at DOI: 10.1021/acsomega.8b02041.

SEM images of the PVA−TA hydrogels (PDF)

■ AUTHOR INFORMATION

Corresponding Author

*E-mail: wanghl@bnu.edu.cn (H.W.).

ORCID

Huiliang Wang: 0000-0001-7964-0809

Author Contributions

The manuscript was written through contributions of all authors. All authors have given approval to the final version of the manuscript.

Notes

The authors declare no competing financial interest.

■ ACKNOWLEDGMENTS

This work was financially supported by the National Natural Science Foundation of China (grant no. 21274013), the Fundamental Research Funds for the Central Universities, and the Program for Changjiang Scholars and Innovative Research Team in University (PCSIRT).

■ REFERENCES

(1) Haque, M. A.; Kurokawa, T.; Gong, J. P. Super tough double network hydrogels and their application as biomaterials. *Polymer* **2012**, *53*, 1805−1822.

(2) Hoffman, A. S. Hydrogels for biomedical applications. *Adv. Drug Delivery Rev.* **2012**, *64*, 18−23.

(3) Richter, A.; Paschew, G.; Klatt, S.; Lienig, J.; Arndt, K.-F.; Adler, H.-J. Review on hydrogel-based pH sensors and microsensors. *Sensors* **2008**, *8*, 561−581.

(4) Jiang, F.; Huang, T.; He, C.; Brown, H. R.; Wang, H. Interactions affecting the mechanical properties of macromolecular microsphere composite hydrogels. *J. Phys. Chem. B* **2013**, *117*, 13679−13687.

DOI: 10.1021/acsomega.8b02041
ACS Omega 2018, 3, 11788−11795

(5) Um, S. H.; Lee, J. B.; Park, N.; Kwon, S. Y.; Umbach, C. C.; Luo, D. Enzyme-catalysed assembly of DNA hydrogel. *Nat. Mater.* **2006**, *5*, 797−801.
(6) Okay, O. DNA Hydrogels: New functional soft materials. *J. Polym. Sci., Part B: Polym. Phys.* **2011**, *49*, 551−556.
(7) Zhu, J.; Wang, X.; He, C.; Wang, H. Mechanical properties, anisotropic swelling behaviours and structures of jellyfish mesogloea. *J. Mech. Behav. Biomed. Mater.* **2012**, *6*, 63−73.
(8) Smith, A. M.; Williams, R. J.; Tang, C.; Coppo, P.; Collins, R. F.; Turner, M. L.; Saiani, A.; Ulijn, R. V. Fmoc-Diphenylalanine Self Assembles to a Hydrogel via a Novel Architecture Based on π-π Interlocked β-Sheets. *Adv. Mater.* **2008**, *20*, 37−41.
(9) Shen, J.-S.; Cai, Q.-G.; Jiang, Y.-B.; Zhang, H.-W. Anion-triggered melamine based self-assembly and hydrogel. *Chem. Commun.* **2010**, *46*, 6786−6788.
(10) Xu, Y.; Sheng, K.; Li, C.; Shi, G. Self-assembled graphene hydrogel via a one-step hydrothermal process. *ACS Nano* **2010**, *4*, 4324−4330.
(11) Yu, P.; Bao, R.-Y.; Shi, X.-J.; Yang, W.; Yang, M.-B. Self-assembled high-strength hydroxyapatite/graphene oxide/chitosan composite hydrogel for bone tissue engineering. *Carbohydr. Polym.* **2017**, *155*, 507−515.
(12) Umbreen, N.; Sohni, S.; Ahmad, I.; Khattak, N. U.; Gul, K. Self-assembled three-dimensional reduced graphene oxide-based hydrogel for highly efficient and facile removal of pharmaceutical compounds from aqueous solution. *J. Colloid Interface Sci.* **2018**, *527*, 356−367.
(13) Li, Z.; Deming, T. J. Tunable hydrogel morphology via self-assembly of amphiphilic pentablock copolypeptides. *Soft Matter* **2010**, *6*, 2546−2551.
(14) Frohm, B.; DeNizio, J. E.; Lee, D. S. M.; Gentile, L.; Olsson, U.; Malm, J.; Åkerfeldt, K. S.; Linse, S. A peptide from human semenogelin I self-assembles into a pH-responsive hydrogel. *Soft Matter* **2015**, *11*, 414−421.
(15) Nowak, A. P.; Breedveld, V.; Pakstis, L.; Ozbas, B.; Pine, D. J.; Pochan, D.; Deming, T. J. Rapidly recovering hydrogel scaffolds from self-assembling diblock copolypeptide amphiphiles. *Nature* **2002**, *417*, 424−428.
(16) Chiang, P.-R.; Lin, T.-Y.; Tsai, H.-C.; Chen, H.-L.; Liu, S.-Y.; Chen, F.-R.; Hwang, Y.-S.; Chu, I.-M. Thermosensitive hydrogel from oligopeptide-containing amphiphilic block copolymer: effect of peptide functional group on self-assembly and gelation behavior. *Langmuir* **2013**, *29*, 15981−15991.
(17) Wang, H.; Paul, A.; Nguyen, D.; Enejder, A.; Heilshorn, S. C. Tunable control of hydrogel microstructure by kinetic competition between self-assembly and crosslinking of elastin-like proteins. *ACS Appl. Mater. Interfaces* **2018**, *10*, 21808−21815.
(18) Wan, L.; Chen, Q.; Liu, J.; Yang, X.; Huang, J.; Li, L.; Guo, X.; Zhang, J.; Wang, K. Programmable self-assembly of DNA-protein hybrid hydrogel for enzyme encapsulation with enhanced biological stability. *Biomacromolecules* **2016**, *17*, 1543−1550.
(19) Mehl, A. F.; Feer, S. P.; Cusimano, J. S. Hydrogel biopolymer created from the self-assembly of a designed protein containing a four-helix bundle forming motif. *Biomacromolecules* **2012**, *13*, 1244−1249.
(20) Lao, U. L.; Sun, M.; Matsumoto, M.; Mulchandani, A.; Chen, W. Genetic engineering of self-assembled protein hydrogel based on elastin-like sequences with metal binding functionality. *Biomacromolecules* **2007**, *8*, 3736−3739.
(21) Zhang, L.; Lei, J.; Liu, L.; Li, C.; Ju, H. Self-assembled DNA hydrogel as switchable material for aptamer-based fluorescent detection of protein. *Anal. Chem.* **2013**, *85*, 11077−11082.
(22) Xiang, B.; He, K.; Zhu, R.; Liu, Z.; Zeng, S.; Huang, Y.; Nie, Z.; Yao, S. Self-assembled DNA hydrogel based on enzymatically polymerized DNA for protein encapsulation and enzyme/DNAzyme hybrid cascade reaction. *ACS Appl. Mater. Interfaces* **2016**, *8*, 22801−22807.
(23) Lu, S.; Wang, S.; Zhao, J.; Sun, J.; Yang, X. A pH-controlled bidirectionally pure DNA hydrogel: reversible self-assembly and fluorescence monitoring. *Chem. Commun.* **2018**, *54*, 4621−4624.
(24) Huang, Z.; Kangovi, G. N.; Wen, W.; Lee, S.; Niu, L. An RNA aptamer capable of forming a hydrogel by self-assembly. *Biomacromolecules* **2017**, *18*, 2056−2063.
(25) Joo, V.; Ramasamy, T.; Haidar, Z. S. A Novel Self-assembled liposome-based polymeric hydrogel for cranio-maxillofacial applications: Preliminary findings. *Polymers* **2011**, *3*, 967−974.
(26) Dai, H.; Li, X.; Long, Y.; Wu, J.; Liang, S.; Zhang, X.; Zhao, N.; Xu, J. Multi-membrane hydrogel fabricated by facile dynamic self-assembly. *Soft Matter* **2009**, *5*, 1987−1989.
(27) Huang, K.; Li, L.; Wang, J.; Zhou, Z.; Guo, X. Tunable double-stranded inclusion complexes of γ-cyclodextrin threaded onto non-modified poly(ethylene glycol). *Colloid Polym. Sci.* **2016**, *294*, 311−319.
(28) Gao, J.; Tang, C.; Elsawy, M. A.; Smith, A. M.; Miller, A. F.; Saiani, A. Controlling self-assembling peptide hydrogel properties through network topology. *Biomacromolecules* **2017**, *18*, 826−834.
(29) Vemula, P. K.; Kohler, J. E.; Blass, A.; Williams, M.; Xu, C.; Chen, L.; Jadhav, S. R.; John, G.; Soybel, D. I.; Karp, J. M. Self-assembled hydrogel fibers for sensing the multi-compartment intracellular milieu. *Sci. Rep.* **2014**, *4*, 4466.
(30) Wickremasinghe, N. C.; Kumar, V. A.; Hartgerink, J. D. Two-step self-assembly of liposome-multidomain peptide nanofiber hydrogel for time-controlled release. *Biomacromolecules* **2014**, *15*, 3587−3595.
(31) Sun, N.; Wang, T.; Yan, X. Self-assembled supermolecular hydrogel based on hydroxyethyl cellulose: Formation, in vitro release and bacteriostasis application. *Carbohydr. Polym.* **2017**, *172*, 49−59.
(32) Marchesan, S.; Qu, Y.; Waddington, L. J.; Easton, C. D.; Glattauer, V.; Lithgow, T. J.; McLean, K. M.; Forsythe, J. S.; Hartley, P. G. Self-assembly of ciprofloxacin and a tripeptide into an antimicrobial nanostructured hydrogel. *Biomaterials* **2013**, *34*, 3678−3687.
(33) Hassan, C. M.; Peppas, N. A. Structure and morphology of freeze/thawed PVA hydrogels. *Macromolecules* **2000**, *33*, 2472−2479.
(34) Zhang, L.; Zhao, J.; Zhu, J.; He, C.; Wang, H. Anisotropic tough poly(vinyl alcohol) hydrogels. *Soft Matter* **2012**, *8*, 10439−10447.
(35) Hong, K. H. Preparation and properties of polyvinyl alcohol/tannic acid composite film for topical treatment application. *Fibers Polym.* **2016**, *17*, 1963−1968.
(36) Lomas, H.; Johnston, A. P. R.; Such, G. K.; Zhu, Z.; Liang, K.; Van Koeverden, M. P.; Alongkornchotikul, S.; Caruso, F. Polymersome-loaded capsules for controlled release of DNA. *Small* **2011**, *7*, 2109−2119.
(37) Zhou, L.; Chen, M.; Tian, L.; Guan, Y.; Zhang, Y. Release of polyphenolic drugs from dynamically bonded layer-by-layer films. *ACS Appl. Mater. Interfaces* **2013**, *5*, 3541−3548.
(38) Chen, J.; Ratnayaka, S.; Alford, A.; Kozlovskaya, V.; Liu, F.; Xue, B.; Hoyt, K.; Kharlampieva, E. Theranostic multilayer capsules for ultrasound imaging and guided drug delivery. *ACS Nano* **2017**, *11*, 3135−3146.
(39) Kozlovskaya, V.; Kharlampieva, E.; Drachuk, I.; Cheng, D.; Tsukruk, V. V. Responsive microcapsule reactors based on hydrogen-bonded tannic acid layer-by-layer assemblies. *Soft Matter* **2010**, *6*, 3596−3608.
(40) Zhao, Y.-N.; Gu, J.; Jia, S.; Guan, Y.; Zhang, Y. Zero-order release of polyphenolic drugs from dynamic, hydrogen-bonded LBL films. *Soft Matter* **2016**, *12*, 1085−1092.
(41) Krogsgaard, M.; Andersen, A.; Birkedal, H. Gels and threads: mussel-inspired one-pot route to advanced responsive materials. *Chem. Commun.* **2014**, *50*, 13278−13281.
(42) Fan, H.; Wang, J.; Zhang, Q.; Jin, Z. Tannic acid-based multifunctional hydrogels with facile adjustable adhesion and cohesion contributed by polyphenol supramolecular chemistry. *ACS Omega* **2017**, *2*, 6668−6676.
(43) Shin, M.; Ryu, J. H.; Park, J. P.; Kim, K.; Yang, J. W.; Lee, H. DNA/tannic acid hybrid gel exhibiting biodegradability, extensibility, tissue adhesiveness, and hemostatic ability. *Adv. Funct. Mater.* **2015**, *25*, 1270−1278.

DOI: 10.1021/acsomega.8b02041
ACS Omega 2018, 3, 11788−11795

(44) Fan, H.; Wang, L.; Feng, X.; Bu, Y.; Wu, D.; Jin, Z. Supramolecular hydrogel formation based on tannic acid. *Macromolecules* **2017**, *50*, 666−676.
(45) Xu, R.; Ma, S.; Lin, P.; Yu, B.; Zhou, F.; Liu, W. High strength astringent hydrogels using protein as the building block for physically cross-linked multi-network. *ACS Appl. Mater. Interfaces* **2018**, *10*, 7593−7601.
(46) Hong, K. H. Polyvinyl alcohol/tannic acid hydrogel prepared by a freeze-thawing process for wound dressing applications. *Polym. Bull.* **2017**, *74*, 2861−2872.
(47) Chen, Y.-N.; Peng, L.; Liu, T.; Wang, Y.; Shi, S.; Wang, H. Poly(vinyl alcohol)-tannic acid hydrogels with excellent mechanical properties and shape memory behaviors. *ACS Appl. Mater. Interfaces* **2016**, *8*, 27199−27206.
(48) Pretsch, E.; Bühlmann, P.; Affolter, C. *Structure Determination of Organic Compounds: Tables of Spectral Data*, 4th ed.; Springer: Berlin, 2000; p 287.
(49) Ricciardi, R.; Auriemma, F.; De Rosa, C.; Lauprêtre, F. X-ray diffraction analysis of poly(vinyl alcohol) hydrogels, obtained by freezing and thawing techniques. *Macromolecules* **2004**, *37*, 1921−1927.
(50) Shi, S.; Peng, X.; Liu, T.; Chen, Y.-N.; He, C.; Wang, H. Facile preparation of hydrogen-bonded supramolecular polyvinyl alcohol-glycerol gels with excellent thermoplasticity and mechanical properties. *Polymer* **2017**, *111*, 168−176.

DOI: 10.1021/acsomega.8b02041
ACS Omega 2018, 3, 11788−11795